

# Dynamic equivalent of wind farm model for power system stability studies

Maharajan Duraisamy, Kumudini Devi Raguru Pandu & Ramanujam Rangarajan

To cite this article: Maharajan Duraisamy, Kumudini Devi Raguru Pandu & Ramanujam Rangarajan (2017) Dynamic equivalent of wind farm model for power system stability studies, *Automatika*, 58:2, 216-231, DOI: [10.1080/00051144.2017.1391941](https://doi.org/10.1080/00051144.2017.1391941)

To link to this article: <https://doi.org/10.1080/00051144.2017.1391941>



© 2017 The Author(s). Published by Informa UK Limited, trading as Taylor & Francis Group.



Published online: 15 Nov 2017.



Submit your article to this journal [↗](#)



Article views: 1252



View related articles [↗](#)



View Crossmark data [↗](#)



## Dynamic equivalent of wind farm model for power system stability studies

Maharajan Duraisamy <sup>a</sup>, Kumudini Devi Raguru Pandu<sup>b</sup> and Ramanujam Rangarajan<sup>c</sup>

<sup>a</sup>Research Scholar, Anna University, Guindy, India; <sup>b</sup>Power Systems Engineering Division, Anna University, Guindy, India; <sup>c</sup>Department of Electrical and Electronics Engineering, SRM University, Kattankulathur, India

### ABSTRACT

A new dynamic equivalencing method for stability assessment of a grid-integrated wind farm is proposed in this article. The accuracy of the method is validated for a 34-bus system with 28-unit wind farm connected to Indian utility system. This wind farm consists of several wind turbines of two different ratings. The electrical parameters of the equivalent generator are derived from the mathematical model of the squirrel-cage induction generator. The parameters of the equivalent wind-turbine generator are optimized to yield minimum deviation from the detailed system response using genetic algorithm. The small-signal and transient stability responses of the study system with detail wind farm and equivalent model are simulated using MATLAB. Equivalent model eigenvalues are compared to the centre of inertia based detailed system eigenvalue. In addition, the computed eigenvalues and time-domain responses of the proposed equivalent model, detailed wind farm are compared against weighted model proposed earlier. In most of the investigated cases, the average error of dynamic responses between the proposed equivalent and detailed models are less when compared to weighted model. Thus, the large-signal responses of the proposed equivalent model show superior agreement with detailed system response.

### ARTICLE HISTORY

Received 3 June 2017  
Accepted 9 October 2017

### KEYWORDS

Transient stability; small-signal stability; dynamic equivalent; squirrel-cage induction generator; Indian utility system; wind farm; genetic algorithm

## 1. Introduction

In developing countries like India, the steady state and dynamic operation of the power system are mainly influenced by increased installed capacity of wind generation. Moreover, the power evacuation from the large-scale wind farm (WF) is limited by the low short circuit power of the grid. In the immediate assessment of the stability simulation of such grid integrated WF, an accurate single-equivalent model of the WF is significantly needed. Such an equivalent model is useful in carrying out steady state and dynamic simulation studies that form an integral part of power system planning. Grid code standards and requirements for integrating the large-scale WF into bulk transmission system are discussed in [1].

The qualitative study of simple power system with large-scale wind power penetration is investigated in [2]. It was found that the impact of wind power mainly contributes damping. The power oscillation damping effect is improved particularly when squirrel-cage induction generators (SCIGs) are used.

Most of the WFs in India guise tree-like structure in which the wind-turbine generators (WTGs) of different ratings are mixed. In such case, simple aggregation of the WF yields inaccurate solution [3,4]. Identical WTGs with same operational points of WTG in a WF is assumed. The effect of equivalent network impedance is not included in the equivalent WTG. Multi-turbine

equivalent model suggested for an irregular wind distribution over the large area of the WF. Aggregation technique used to develop an equivalent model for the fixed speed WTG-based WF developed in [5] includes the swing equations, the impedance of the generator transformer and generator impedances. In addition, the injected real power by the aggregated model has more error compared to detail model under transient condition. This is due to that fact the aggregated model does not accounting the feeder impedance between WTG to point of common coupling (PCC) point.

A method of aggregating fixed speed-wind-turbine generators (FSWTGs) based WF is studied in [6] and yields two equivalent WTGs. In the case of uniform wind distribution in the WF, a simple equivalent model is used. In addition a refined model is also suggested to take into account non-uniform wind speed. At PCC, the responses of variable single equivalent with compensating capacitor model approximately matches with the detailed system.

Single-equivalent model of WF that consists of fixed speed WTGs is developed in [7] and the simulated results are validated against the field measurements. Short- and long-time frame simulations have been taken for comparison and the error between aggregated and detailed models becomes larger if all the WTGs are operated at different operating conditions. In this equivalent model, the mechanical input power is assumed to be constant. Also, mechanical

parameters used in the simulation are inaccurate [7]. However, in the case of non-uniform wind velocity in large-scale WF, some of the WTGs are tripped due to high/low velocity of wind and the single-equivalent model cannot be used in such event. Analytical approach used in the article [8] is to derive the equivalent (collector) impedance by equating the losses within the detailed WF branch to the total losses of equivalent line/cable. However, all turbines are assumed to be operating in the same point. An aggregated model was developed for the mixed WF with SCIG and doubly fed induction generator (DFIG) as reported in [9]. However, the method for obtaining the equivalent model generator parameters is not straightforward. According to this, genetic algorithm-based optimization is used to minimize the error between the responses of equivalent single generator model and detailed WF. Also, the response of equivalent model is compared with weighted equivalent model reported in the earlier literature [10].

The dynamic equivalent model is developed in order to improve the operating efficiency of WF [11]. Using phasor measurement unit (PMU), the data are obtained from the WF and equivalent model of the WF is derived from parameter identification technique. However, the equivalent model parameters are optimized based on stochastic approximation. An equivalent WF model was developed from synchro-phasor measurement data by the use of parameter identification technique discussed in [12]. The improved genetic algorithm (GA) was employed to develop the equivalent WF for preserving the basic structure, characteristics and control patterns of actual WF. Using the deterministic data, the dynamic multi-machine equivalent modelling of WF is developed [13].

In summary, the methods in [3–9] suggest an aggregated model of similar type with identical rating. Also the equivalent generator parameter just used the re-scaled value of WTGs in the WF. The aggregation method proposed here yields the equivalent system dynamic parameters. It can reduce the system order and simulation time considerably. The method proposed here is based on aggregation technique adopted in [14]. In this reference, several induction motors in an industrial power plant are aggregated to yield a single equivalent which is valid for dynamic conditions. Here, this method is extended to WTG system using SCIG which involves Kron's reduction technique.

The major advantages of this proposed method are as follows:

- (1) WF of any network topology can be aggregated using this method. Most of the methods fail, if meshed topology or any complex network is opted for WF.
- (2) WF consisting of different ratings of generators can be aggregated as single equivalent. In other aggregation methods, if the WF consists of different ratings, multiple clusters are formed and it is represented as multiple equivalents. But simple aggregation of WF is applicable only for identical WTGs.
- (3) Equivalent parameters are accurately obtained from the available parameters of detailed WF.
- (4) The electrical parameters are obtained such that it is operated in steady state; the generation produced by the aggregate model is identical to that of the detail WF model.
- (5) The mechanical parameters of the equivalent WF model are optimized to match the dynamic performance of the model with that of the detailed WF. GA is used in this optimization process.

The paper is organized as follows. Section 2 briefly describes the modelling of the synchronous generator (SG) and the WTG components. In addition, the modelling of two-mass model and wake effect are included. A brief description of the WF considered for investigation is presented in Section 3. The aggregation process to yield the single equivalent based on weighted model method and proposed method are explained in Section 4 and Section 5, respectively. Eigenvalues and time-domain responses of the study system with detail WF representation, proposed equivalent and weighted model reported in [10] are compared in Section 6. Finally, Section 7 concludes the paper.

## 2. Modelling of synchronous generator and WTG components

This section presents the modelling of SG and WTG. The modelling of the SG can be found in detail in [15–18]. The major components of the FSWTG are wind turbine, gear box and SCIG. These are briefly explained in this section. Furthermore, the modelling of wind speed and wake effect is also presented.

### 2.1 Modelling of synchronous generator

The dynamic modelling of SG is cast in direct and quadrature coordinates rotating at synchronous speed [15,16]. The classical model of the SGs is taken for study, so rotor angle and rotor speed of SG are state variables:

$$p\delta_{sgi} = \omega_{sgi} - \omega_s \quad (1)$$

$$p\omega_{sgi} = \frac{1}{2H_{si}} [T_{sgmi} - T_{sgei} - D_{sgi}(\omega_{sgi} - \omega_s)]. \quad (2)$$

The electric torque of the synchronous machine is expressed by

$$T_{sgei} = E'_{sgdi}I_{di} + E'_{sgqi}I_{qi}. \quad (3)$$

The stator algebraic equations are represented as follows:

$$\begin{aligned} E'_{sgdi} - V_i \sin(\delta_{sgi} - \theta_{bi}) - R_{sgi}I_{di} + X'_{qi}I_{qi} &= 0 \\ E'_{sgqi} - V_i \cos(\delta_{sgi} - \theta_{bi}) - R_{sqi}I_{qi} - X'_{di}I_{di} &= 0. \end{aligned} \quad (4)$$

For  $i = 1, \dots, n_{sg}$ , where  $n_{sg}$  is number of SGs

## 2.2 Modelling of wind turbine

An aerodynamic rotor model gives the relationship between the mechanical power of the wind turbine to the rotational speed. The power coefficient ( $C_p$ ) is decided by the tip speed ratio ( $\lambda$ ) and pitch angle ( $\phi$ ). In this paper, the detailed WF has 200 kW and 250 kW FSWTGs with passive stall technique for controlling the speed of the turbine. Hence, the pitch angle control is not included in this model. The tip-speed ratio is given by

$$\lambda = \frac{R\omega_r}{U_w}. \quad (5)$$

The wind turbine captures the wind energy through the blades, and delivers mechanical power ( $P_{wt}$ ) to the shaft. The power extracted from the wind varies as the cube of wind speed and is expressed as

$$P_{wt}(U_w, C_p) = \frac{1}{2} \rho A U_w^3 C_p(\lambda, \phi). \quad (6)$$

The mechanical torque ( $T_m$ ) of wind turbine is given by

$$T_m(U_w, C_p) = \frac{\frac{1}{2} \rho A U_w^3 C_p(\lambda, \phi)}{\omega_t}. \quad (7)$$

The power coefficient  $C_p$  is

$$C_p(\lambda, \phi) = C_1 \left( \frac{C_2}{\Lambda} - C_3\phi - C_4\phi^x - C_5 \right) e^{\left( \frac{-C_6}{\Lambda} \right)}, \quad (8)$$

where

$$\frac{1}{\Lambda} = \frac{1}{\lambda + 0.08\phi} - \frac{0.035}{1 + \phi^3}. \quad (9)$$

The  $C_p$  versus  $\lambda$  and power curve of a wind turbine are provided by the manufacturer. The values of wind wheel coefficients,  $C_1$  to  $C_6$ , the exponent  $x$  and pitch angle  $\phi$  are given in the Appendix.

## 2.3 Modelling of squirrel-cage induction generator

SCIG is employed for wind power generation because of its simple construction and ruggedness. The dynamic modelling of induction generator is cast in direct and

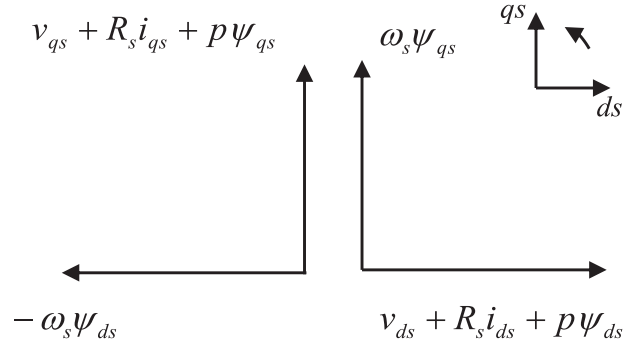


Figure 1. Two-axis diagram for the stator  $dq$ -axis voltage equations of SCIG.

quadrature coordinates rotating at synchronous speed [15,16]. Three-phase stator and rotor voltage equations are referred to synchronously rotating reference frame with quadrature axis ( $q$ -axis) leading direct axis ( $d$ -axis) by  $90^\circ$ . Generator convention is used, i.e. stator current and rotor current are considered to be positive when they are leaving and entering the machine, respectively.

The stator  $dq$  voltage equations are shown in Figure 1, the two-axis diagram [17,18] forms relationship between terminal voltage, speed emf and resistive drop. The diagram for the rotor is obtained by replacing the stator quantities by corresponding rotor quantities and  $\omega_s$  by  $\omega_s - \omega_r$ .

The per unit stator and rotor  $dq$ -axis voltage equations of SCIG are as follows:

$$v_{ds} = -R_s i_{ds} + \omega_s \psi_{qs} - p \psi_{ds} \quad (10)$$

$$v_{qs} = -R_s i_{qs} - \omega_s \psi_{ds} - p \psi_{qs} \quad (11)$$

$$v_{dr} = -R_r i_{dr} + s \omega_s \psi_{qr} - p \psi_{dr} \quad (12)$$

$$v_{qr} = -R_r i_{qr} - s \omega_s \psi_{dr} - p \psi_{qr}. \quad (13)$$

The per unit stator and rotor  $dq$ -axis flux linkage equations are as follows:

$$\psi_{ds} = L_s i_{ds} + L_m i_{dr} \quad (14)$$

$$\psi_{qs} = L_s i_{qs} + L_m i_{qr} \quad (15)$$

$$\psi_{dr} = L_r i_{dr} + L_m i_{ds} \quad (16)$$

$$\psi_{qr} = L_r i_{qr} + L_m i_{qs}. \quad (17)$$

The third-order model for the induction generator is considered with the following assumptions.

- (1) The stator transients are negligible, which implies  $p \psi_{ds}$  and  $p \psi_{qs}$  terms are zero in Equations (10) and (11).
- (2) The rotor is short circuited which implies that  $v_{dr}$  and  $v_{qr}$  are zero in Equations (12) and (13).
- (3) The transient  $dq$ -axis rotor voltages are given by

$$E'_{ds} = \frac{X_m}{L_r} \psi_{qr} \quad (18)$$

and

$$E'_{qs} = -\frac{X_m}{L_r} \psi_{dr}. \quad (19)$$

The transient reactance ( $X'_s$ ) is given by

$$X'_s = X_s - \frac{X_m^2}{X_r}. \quad (20)$$

The differential equations of the third-order model of SCIG are given by

$$pE'_{ds} = -\frac{1}{T_o'} [E'_{ds} - (X_s - X'_s)i_{qs}] + s\omega_s E'_{qs} \quad (21)$$

$$pE'_{qs} = -\frac{1}{T_o'} [E'_{qs} + (X_s - X'_s)i_{ds}] - s\omega_s E'_{ds}, \quad (22)$$

where the rotor open circuit time constant is  $T_o' = L_r/R_r$ .

The expression for electromagnetic torque is

$$T_e = \psi_{ds}i_{qs} - \psi_{qs}i_{ds}. \quad (23)$$

## 2.4 Model of drive train

The drive train of the wind turbine is represented by a two-mass model as shown in Figure 2 and is described by the following equations: (for more details see [19]):

$$p\omega_t = \frac{1}{2H_t} [T_m(U_w, C_p) - T_{sh}] \quad (24)$$

$$p\delta_{wt} = \omega_t - \omega_r \quad (25)$$

$$p\omega_r = \frac{1}{2H_g} (T_{sh} - T_e), \quad (26)$$

where

$$T_{sh} = K_{sh}\delta_{wt} + D_{sh}(\omega_t - (1-s)\omega_s). \quad (27)$$

## 2.5 Modelling of wind speed

Generally, wind speed is intermittent and stochastic in nature. The mechanical torque produced by WTG is directly proportional to the wind speed. Hence, the suitable wind speed model must be taken into account to simulate WTG dynamics. The four-component

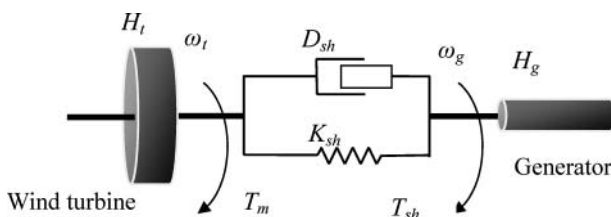


Figure 2. Two-mass model of wind-turbine generator.

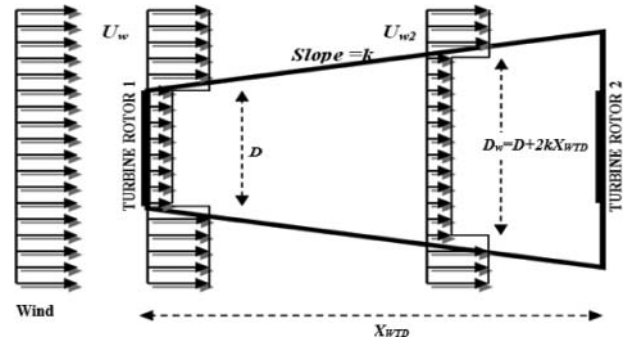


Figure 3. Simple wake model.

wind speed model is chosen in this paper [4] and defined as

$$U_w(t) = U_a + U_r(t) + U_g(t) + U_{tc}(t). \quad (28)$$

## 2.6 Modelling of wake effect

A simple wake effect model is illustrated as shown in Figure 3 [20,21]. According to this model given by Equation (29) the wind speed seen by the turbine rotor 2 in row-2 is decreased, thereby affecting the power generation of row-2 WTGs installed within the wake region as shown in Figure 3:

$$U_{w2}(t) = U_w(t) \left[ 1 - \left( 1 - \sqrt{(1 - C_t)} \right) \left[ \frac{D}{D + 2kX_{WTD}} \right]^2 \right]. \quad (29)$$

## 3. Detailed WF system

The WF considered for investigation is located in Kayathar, Tamil Nadu state, India, with a total installed capacity of 5.85 MW. The WF is connected at bus 8, PCC of 34-bus system shown in Figure 4. It can be seen that the detail WF is given in Figure 5 which shows 28 numbers of WTGs arranged in 3 rows. The generators in the first row encounter higher wind speed and the speed decreases as we go down the rows, taking wake effect into consideration. The 200-kW wind generator is considered in second row except one which is rated of 250 kW. The rating of each SG is 250 MVA and load 1 is connected at bus 5 and load 2 at bus 6 with each capacity of real power 100 MW and reactive power of 40 MVar. Grid is represented as SG in dynamic simulation. SG data are found in [18]. The data of study system are given in the Appendix (Tables A.1–A.3).

The data for the equivalent system model are derived from the detailed representation of the WF. At bus 8, the entire WF is represented by the single-equivalent model as shown in Figure 6.



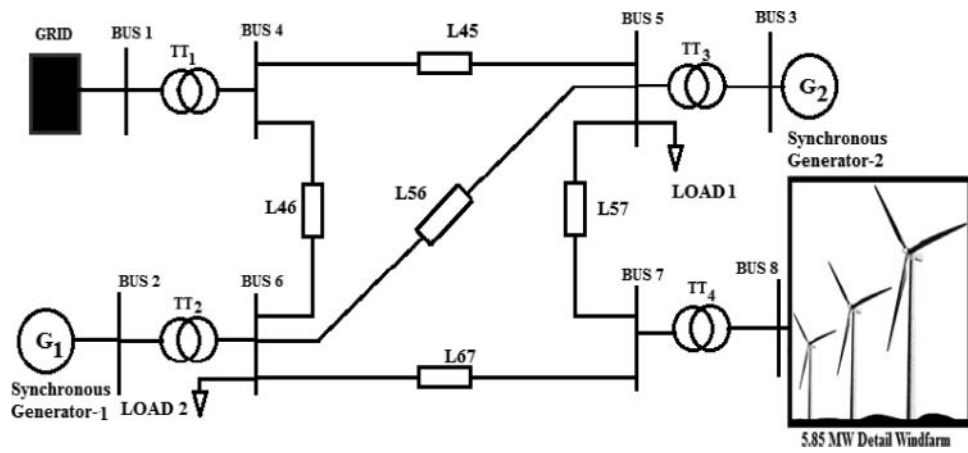


Figure 4. Single-line diagram of the study system.

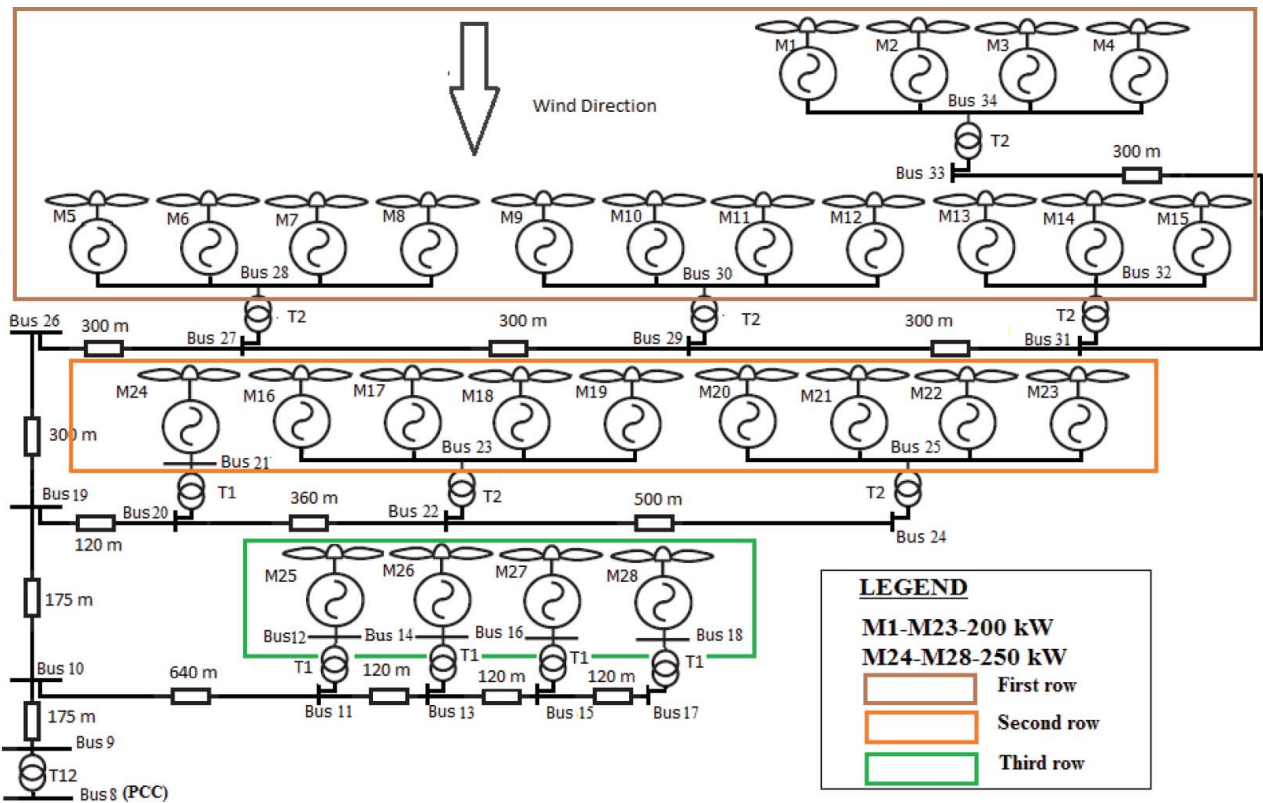


Figure 5. Single-line diagram of the detailed wind farm (bus 8 to bus 34).

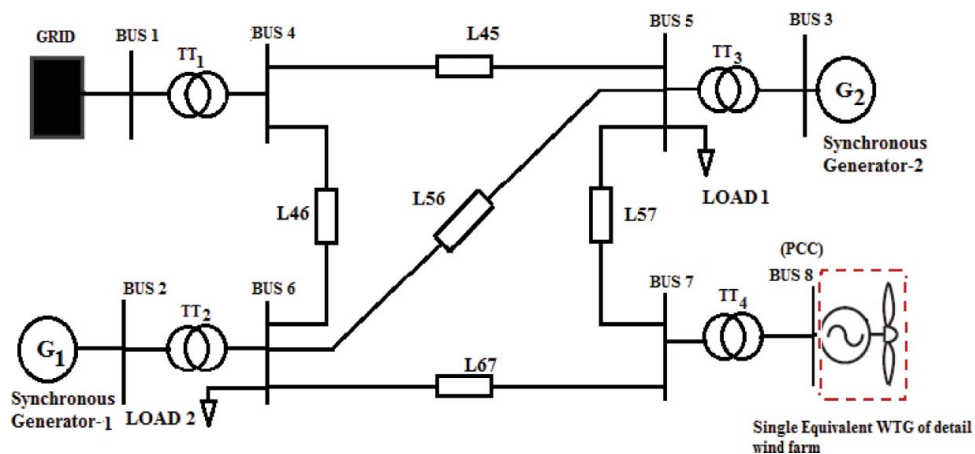


Figure 6. Single-line diagram of the study system with single equivalent of detail wind farm.

#### 4. Weighted model equivalent of wind farm

Weighted-model-based equivalent method gives the simplest representation of aggregated WF model with acceptable precision in power system stability studies reported in [10]. Wind turbine facing same wind velocity can be grouped together and it can be represented as a single aggregate wind turbine model or an equivalent generator model.

The salient points that are discussed in the weighted model in reference [10] are as follows:

- (1) The first-, third- and fifth-order WTG models in the WF are compared (Electromagnetic transient) for the EMT type simulation using software packages PSS/E and PSCAD/EMTDC.
- (2) In this method, all the WTGs in the WF are considered as identically rated. According to this method, the equivalent generator parameters are obtained based on scaled down values of WTG in a WF.
- (3) The WF's internal network influences on dynamic studies are considered. The developed new equivalent WF model from detailed WF enables weighted average values of voltages at each WTG. The weighted average of voltage drop is calculated based on real power flow on the lines and depends on WTG connection (series or parallel) within a WF.
- (4) In addition, the line susceptance effect is neglected in the equivalent generator's line impedance calculation. In time-domain simulation studies, the damping coefficient of WTG is not accounted for the derived weighted equivalent model.
- (5) Weighted average model is modified and applied to aggregation of type-4 WTG (PMSG-based fully rated converter WTG) based WF investigated in [22] and the model used includes both stability, EMT type simulation studies.

However, the voltage drop across the line is depending on the real power flow as well as reactive power flow. Also, the equivalent weighted model's line impedance calculation is not straightforward because the WTG connection in detailed WF should be known prior whether it is connected in series or parallel. The wind speed variation in the WF is not considered. Also, wake effect model is not included in the equivalent WTG. In the proposed method the equivalent line impedance of the WF retained in the equivalent generator parameters through Kron's reduction. Furthermore, in this work, the stability investigation of detailed and equivalent WTG models is performed with wake effect. The methodology for obtaining the proposed dynamic equivalent model of WF is discussed in the next section.

#### 5. Proposed dynamic equivalent wind farm model

Dynamic equivalent of WF is constructed in two-fold. First, the equivalent wind turbine model is developed using Equations (30)–(33). Second, the equivalent generator is yielded through modelling of SCIG.

##### 5.1 Wind turbine aggregation

The power rating of the equivalent wind turbine is obtained by adding individual machine wind turbine ratings. The equivalent wind speed ( $U_{we}$ ) is given by

$$U_{we} = \sqrt[3]{\frac{1}{nt} \sum_{i=1}^{nt} U_{wi}^3}. \quad (30)$$

The equivalent generator mechanical power  $P_{WTe}$  is given by

$$P_{WTe} = K_{WTe} U_{we}^3, \quad (31)$$

where  $K_{WTe}$  is equivalent generator power constant given by

$$K_{WTe} = \sum_{i=1}^{nt} \frac{1}{2} \rho A_i C_{pi}(\lambda, \phi). \quad (32)$$

The equivalent WTG's compensating capacitor ( $C_e$ ), turbine inertia constant ( $H_{te}$ ), generator inertia constant ( $H_{ge}$ ), stiffness constant ( $K_{she}$ ) and damping constant ( $D_{she}$ ) are calculated as follows:

$$\left. \begin{aligned} C_e &= \sum_{i=1}^{nt} C_i; & H_{te} &= \sum_{i=1}^{nt} H_{ti}; \\ H_{ge} &= \sum_{i=1}^{nt} H_{gi}; & K_{she} &= \sum_{i=1}^{nt} K_{shi}; \\ D_{she} &= \sum_{i=1}^{nt} D_{shi} \end{aligned} \right\} \quad (33)$$

The compensating capacitor of the equivalent generator  $C_e$  is included in the admittance matrix.

##### 5.2 Equivalent generator model electrical parameters

WTGs are represented by fifth-order model using Equations (21), (22) and Equations (24)–(27) for detailed WF system, as shown in Figure 5. Bus admittance matrix is constructed for the study system shown in Figure 4. Kron's reduction is applied to admittance matrix  $[Y]$  to get the equivalent generator transient reactance.

The individual generator transformers and inter-connecting lines of the detailed WF are included in the admittance matrix  $[Y]$  given by

$$[Y] = \begin{bmatrix} Y_{RR} & Y_{RE} \\ Y_{ER} & Y_{EE} \end{bmatrix}. \quad (34)$$

The transient admittance of the individual generators is absorbed in the diagonals of  $[Y]$  which is reduced to yield the admittance  $\frac{1}{R_s + jX'_s}$  of the equivalent generator. Thus, we have

$$R_s + jX'_s = \frac{1}{[Y_{RR}] - [Y_{RE}][Y_{EE}]^{-1}[Y_{ER}]}. \quad (35)$$

The SCIG model is used to derive the other parameters of the equivalent generator.

At the PCC (bus 8) in [Figure 4](#), the real power generated and reactive power absorbed by the detail WF at the rated wind speed are represented as  $P$  and  $Q$ . Using  $P$  and  $Q$ , the equivalent generator power factor angle,  $\theta$  can be obtained as

$$\theta = \tan^{-1}(Q/P). \quad (36)$$

For the equivalent SCIG, voltage behind transient reactance is given by

$$\overline{E}'_m = \overline{V}_s + (R_s + jX'_s)\overline{I}_s. \quad (37)$$

### 5.3 Procedure to obtain stator reactance of equivalent generator ( $X_s$ )

The steps for arriving at the stator reactance of equivalent generator are given as follows:

**Step 1:** Get the phasor form of the voltage  $p\overline{E}'_m$  using [Equations \(21\)](#) and [\(22\)](#). It is given by

$$p\overline{E}'_m = \left(-\frac{R_r}{X_r} - js\right)\omega_s \overline{E}'_m - j\frac{R_r}{X_r}(X_s - X'_s)\omega_s \overline{I}_s, \quad (38)$$

where

$$\overline{E}'_m = E'_{ds} + jE'_{qs} \quad (39)$$

**Step 2:** For steady-state condition  $p\overline{E}'_m = 0$ . Assume  $X_r \cong X_s$  and setting magnitude of stator current to unity in [Equation \(37\)](#), we can show that

$$\frac{E'_{qs}}{E'_{ds}} = \frac{R_r \cos \theta - sX_r \sin \theta}{R_r \sin \theta + sX_r \cos \theta}. \quad (40)$$

**Step 3:** Setting  $\overline{V}_s = 1$  p.u. and  $\overline{I}_s = \cos \theta - j \sin \theta$  in [Equation \(38\)](#) yields

$$\frac{E'_{qs}}{E'_{ds}} = \frac{X'_s \cos \theta - R_s \sin \theta}{1 + R_s \cos \theta + X'_s \sin \theta}. \quad (41)$$

**Step 4:** Solving [Equations \(40\)](#) and [\(41\)](#) yield [Equation \(42\)](#).

The equivalent SCIG's stator reactance ( $X_s$ ) is given by

$$X_s = \frac{R_r (R_s + \cos \theta)}{s (X'_s + \sin \theta)}. \quad (42)$$

To calculate the stator reactance of the equivalent generator the value of  $(R_r/s)$  has to be known. The procedure for obtaining  $(R_r/s)$  is described below.

### 5.4 Finding the ratio of rotor resistance to full load slip of equivalent generator

The major steps in arriving at the ratio of rotor resistance to full load slip of equivalent generator are as follows:

**Step 1:** Stator current of induction generator from [Equation \(37\)](#) is given by

$$\overline{I}_s = \frac{\overline{E}'_m - \overline{V}_s}{(R_s + jX'_s)}. \quad (43)$$

**Step 2:** Substituting [Equation \(43\)](#) in [Equation \(38\)](#) and considering steady-state condition with 1.0 p.u voltage yield.

$$\overline{E}'_m = \frac{j\frac{R_r}{s}(X_s - X'_s)}{\left(\frac{R_r R_s}{X_r} - X_s X'_s\right) + j\left(\frac{R_r}{s} + R_s\right)X_s}. \quad (44)$$

**Step 3:** Rationalising [Equation \(44\)](#) and using [Equation \(39\)](#), we can obtain

$$\frac{E'_{qs}}{E'_{ds}} = \frac{\frac{R_r R_s}{s} - X_s X'_s}{X_s \left(\frac{R_r}{s} + R_s\right)}. \quad (45)$$

**Step 4:** It is assumed that the equivalent generator is operating at full load with rated speed delivering rated power at unity current magnitude. Solving [Equation \(45\)](#) for  $R_r/s$  yields [Equation \(46\)](#).



The deduced expression of ratio of rotor resistance to full load slip of the equivalent generator is given by

$$\frac{R_r}{s} = \frac{X_s \left( R_s \frac{E'_{qs}}{E_{ds}} + X'_s \right)}{\left( R_s - X_s \frac{E'_{qs}}{E_{ds}} \right)}. \quad (46)$$

When the equivalent generator is operated at full load, the magnitude of slip  $|s|$  is close to  $R_r$  and hence  $|\frac{R_r}{s}|$  becomes unity. Equations (42) and (46) are directly solved for  $X_s$  and  $R_r/s$ .

### 5.5 Determination of operating slip and finding the magnetizing and leakage reactance of the equivalent generator

The aggregated mechanical power is obtained by using Equation (31). The terminal voltage at bus-8 for the equivalent generator is calculated from the steady-state operating conditions of the detailed WF. Therefore, by knowing the mechanical power supplied to the equivalent generator and terminal voltage of the equivalent generator, the slip ( $s$ ) is calculated iteratively from the simple quadratic equation as discussed in [23].

The magnetizing reactance ( $X_m$ ) for the equivalent generator is given by

$$X_m = \sqrt{X_s(X_s - X'_s)}. \quad (47)$$

The leakage reactance ( $X_l$ ) of the equivalent generator is

$$X_l = X_s - X_m. \quad (48)$$

Hence, the known equivalent generator electrical parameters  $R_s$ ,  $R_r/s$ ,  $X_s$ ,  $X_m$  and  $X_l$  are sufficient to mimic the response of the detailed system. The optimization of the equivalent generator parameters is explained in the next section.

### 5.6 Optimization of single-equivalent generator parameters

Development of single-equivalent WF model and its parameters optimization were reported in the earlier literature [24]. The rotor circuit time constant, a moment of inertia and transient reactance of the equivalent generator are taken as control variables for optimization. However, simple WF model is investigated with lumped representation turbine and generator of FSWTG. Also, the SG dynamic influence on WTG is not included in the model.

An optimization method has been used to minimize the error between responses of the detailed WF and single-equivalent model for a dynamic conditions and normal operating condition. Thus, the single-equivalent generator parameters are optimized. The optimization

problem can be solved by using the GA [25]. In this paper, the following control variables are taken for equivalent generator, rotor resistance, inertia of wind turbine, inertia of generator, damping constant of WTG and shaft stiffness. Sum-squared error deviation (SSED) is taken as the main objective function ( $f$ ) with input variables of voltage, real power and reactive power of detailed WF and equivalent generator of WF at the PCC (bus 8) as shown in Figure 4 and Figure 6, respectively.

The optimization problem can be stated as

$$\begin{aligned} \min f = & \sum_{i=1}^N ((P_{Di}^A - P_{Ei})^2 + (Q_{Di}^A - Q_{Ei})^2 \\ & + (V_{Di}^A - V_{Ei})^2). \end{aligned} \quad (49)$$

Subject to equality constraints:

$$\overline{E}_m - \overline{V}_s - (R_s + jX'_s)\overline{I}_s = 0 \quad (50)$$

$$-\left(\frac{R_r}{X_r} + js\right)\omega_s \overline{E}_m - j\frac{R_r}{X_r}(X_s - X'_s)\omega_s \overline{I}_s = 0 \quad (51)$$

$$T_m - T_{sh} = 0; \omega_t - \omega_r = 0; T_{sh} - T_e = 0. \quad (52)$$

For the equivalent generator internal bus, the electrical output mismatch equation is

$$P_E - \text{Re}(\overline{E}_m \overline{I}_s^*) = 0. \quad (53)$$

For the equivalent generator electrical power output and detail system WTG power output mismatch equation is

$$P_{WTe} - \sum_{k=1}^{nt} P_{WTK}(U_w, C_p) = 0, \quad (54)$$

for equivalent generator terminal bus, the real and reactive power mismatch equations are

$$P_E - \text{Re}(\overline{V}_s \overline{I}_s^*) = 0 \quad (55)$$

$$Q_E + \text{Im}(\overline{V}_s \overline{I}_s^*) = 0. \quad (56)$$

Control variables:  $[R_r, H_{te}, H_{ge}, D_{she}, K_{she}]^T$

Control variables limits are:  $R_{rmin} < R_r < R_{rmax}$ ;

$$H_{temin} < H_{te} < H_{temax};$$

$$H_{gemin} < H_{ge} < H_{gemax};$$

$$D_{shemin} < D_{she} < D_{shemax};$$

$$K_{shemin} < K_{she} < K_{shemax};$$

where  $i$  is time step in the non-linear time-domain simulation and  $N$  is the maximum number of time steps. The  $V_D^A, P_D^A, Q_D^A$  and  $V_E, P_E, Q_E$  are variables of the detailed system and equivalent system, respectively. For the each time step, the difference between arrived at detail and equivalent system variables error are squared and added to the fitness function. The objective function

**Table 1.** Study system with detail wind farm and optimized equivalent generator parameters in p.u. (16 MVA base, 11 kV).

Parameters	SCIGs in study system with detailed WF values are in p.u.		WF Equivalent by weighted model values in p.u. [10]	WF Equivalent by proposed model values in p.u.
Machine rating	200 kW	250 kW	5.85 MW	5.85 MW
Stator resistance ( $R_s$ )	0.0031	1.7238	1.92	1.6
Stator reactance ( $X_s$ )	2.4748	2.7308	1.8	1.92
Rotor resistance ( $R_r$ )	19.2011	19.7985	1.92	2.41
Rotor reactance ( $X_r$ )	35.2457	29.4417	34.5	35.3
Magnetizing reactance ( $X_m$ )	512.03	409.62	480	352
Inertia of wind turbine ( $H_t$ )	0.2407	0.2407	6.7392	7.3926
Inertia of wind generator ( $H_g$ )	0.0241	0.0241	0.6752	0.6623
Stiffness constant ( $K_{sh}$ )	0.0575	0.0575	1.6089	1.6529
Damping constant ( $D_{sh}$ )	0.001	0.001	0.0268	0.0311

(49) is minimized by satisfying the equality constraints given by Equations (50)– (55) for non-linear time-domain simulation and the steady-state operating equality constraints given by Equations (53) and (56) of an equivalent generator. The GA-based optimization algorithm is applied to the equivalent systems. The maximum and minimum values of control variables and the parameters of GA are listed in Table A.4. The equivalent generator's rotor resistance ( $R_r$ ), inertia of wind turbine ( $H_{te}$ ), generator ( $H_{ge}$ ), damping co-efficient ( $D_{she}$ ) and stiffness coefficient ( $K_{she}$ ) are chosen as decision variables of the optimization problem. The optimized solution yields the best equivalent model parameters. Optimized equivalent generator parameters are summarized in Table 1.

## 6. System study and results

The proposed equivalent model is validated for small and large disturbances by conducting small-signal and large-signal analysis for the study system shown in Figure 4.

### 6.1 Small-signal model of the study system and equivalent models

To perform the small-signal stability analysis of the study system shown in Figure 4, the small-signal linear model is derived. More details about the development

of state space model of a system are found in reference [26]. In this paper, the classical model of SG and fifth-order model of FSWTG are used for study. The state variables of the complete system are given by

$$X = [\delta_{sg} \omega_{sg} \omega_t^i \delta_{wt}^i \omega_r^i E'_{ds} E'_{qs}]^T,$$

where subscript “sg” denotes SGs variables and superscript “i” refers to induction generator variables.

The state matrix of the study system is obtained by linearizing differential equations and eliminating the algebraic variables as discussed in [26] from Equations (1), (2), Equations (21), (22) and Equations (24–26). Generalized model has been derived analytically

$$\dot{\Delta X} = A_S \Delta X + B_S \Delta U, \quad (57)$$

where  $\Delta X = [\Delta \delta_{sg} \Delta \omega_{sg} \Delta \omega_t^i \Delta \delta_{wt}^i \Delta \omega_r^i \Delta E'_{ds} \Delta E'_{qs}]^T$

$$\Delta U = [\Delta T_{sgm} \Delta T_m^i]^T.$$

The eigenvalues of system are determined from the system matrix  $A_S$  and presented in Tables 2 and 3. The eigenvalues of the study system with detail WF representation, weighted model and proposed equivalent model are presented in Tables 2 and 3.

From Table 2, it can be observed that rotor modes of synchronous machines with WF represented by detailed model are close agreement with proposed equivalent mode than weighted average model.

**Table 2.** Comparison of eigenvalues relevant to SG rotor modes.

SG-1, SG-2, SG-3 (rotor modes)	Study system with detail WF	Study system with WF replaced by weighted model [10]	Study system with WF replaced by proposed equivalent
$\Delta \delta_1^{sg}, \Delta \omega_1^{sg}$	$-0.6923 \pm 11.3933i$	$-0.6945 \pm 11.3957i$	$-0.6935 \pm 11.3946i$
$\Delta \delta_2^{sg}, \Delta \omega_2^{sg}$	$-0.8305 \pm 15.0729i$	$-0.8305 \pm 15.0725i$	$-0.8305 \pm 15.0726i$
$\Delta \delta_3^{sg}, \Delta \omega_3^{sg}$	$-6.9217 \pm 7.5342i$	$-7.3672 \pm 6.6749i$	$-7.0005 \pm 7.3506i$

**Table 3.** Comparison of eigenvalues relevant to detailed, equivalent wind farm models.

WTG modes	Study system with detail WF (COI)	Study system with WF replaced by weighted model [10]	Study system with WF replaced by proposed equivalent
Rotor modes $\Delta \delta_{wt}^i \Delta \omega_r^i$	$-1.8873 \pm 14.8315i^*$	$-3.5915 \pm 20.8858i$	$-1.9507 \pm 14.8665i$
Mechanical mode $\Delta \omega_t^i$	$-0.01356^*$	$-0.0220$	$-0.0136$
Electrical modes $\Delta E'_{ds} \Delta E'_{qs}$	$-0.6580 \pm 0.7623i^*$	$-0.4278 \pm 0.4655i$	$-0.3279 \pm 0.7442i$

\*COI – Centre of inertia of the eigenvalues.

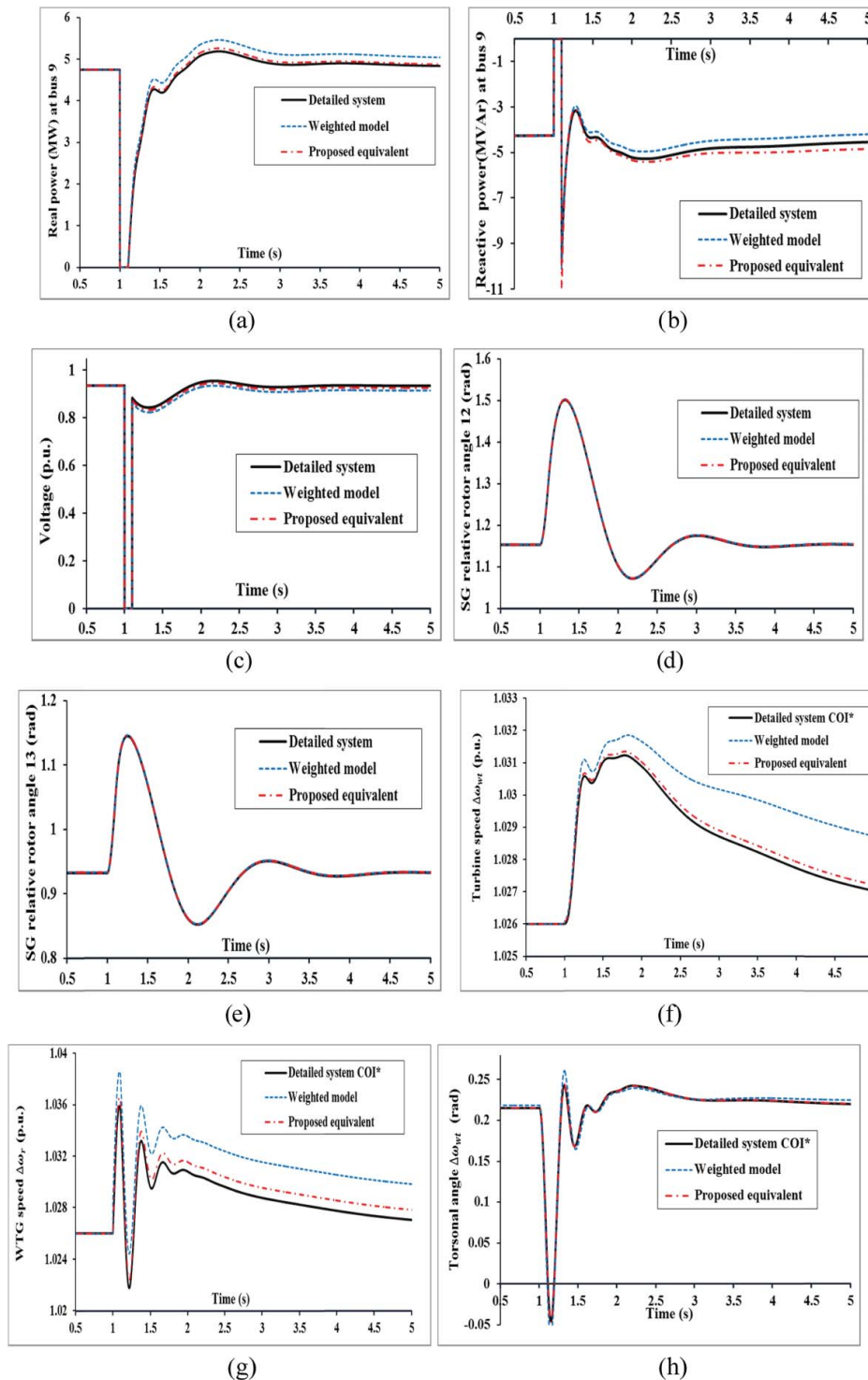


**Figure 7.** Response of the study system and equivalent models at PCC for case 1. (a) Response of real power at bus 8. (b) Response of reactive powers at bus 8. (c) Voltage response at bus 8. (d) Response of Relative rotor angle of SG-2. (e) Response of relative rotor angle of SG-3. (f) Response of wind turbine speed. (g) Response of WT generator speed. (h) Response of WTC torsional angle.

The rotor modes, mechanical mode and electrical modes of the WF models represented in Table 3, eigenvalues of proposed equivalent are matching closely with the detailed WF than weighted average-based equivalent WF model. Therefore, the dynamic equivalent of the WF by proposed equivalent WF system preserves accurately for the given detail system.

## 6.2 Large-signal analysis of the study system and equivalent models

The study system with detailed WF, the WF replaced by weighted model and equivalent systems programmed for transient stability analysis using MATLAB [27] and their dynamic responses are compared.

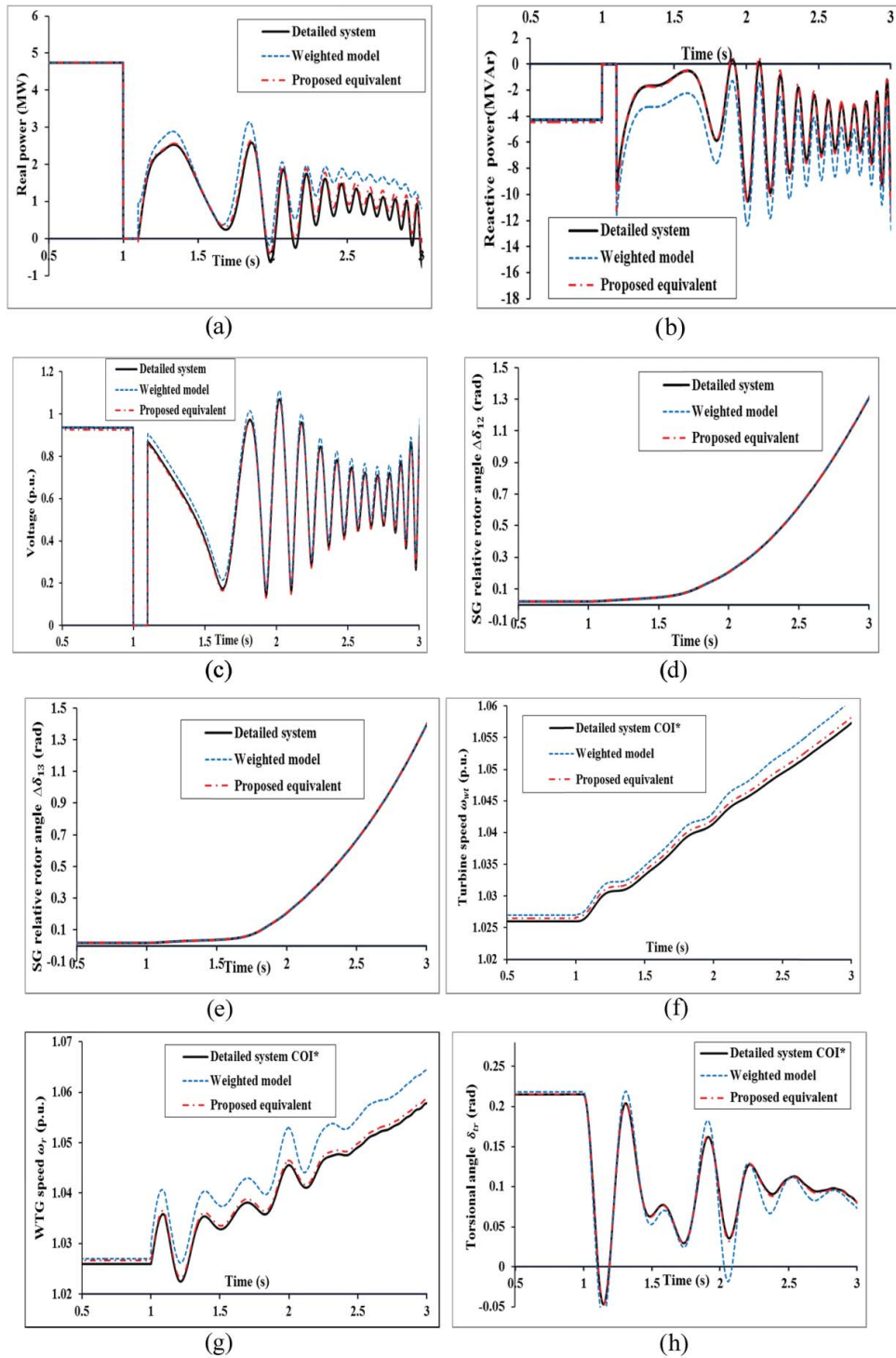


**Figure 8.** Response of the study system and equivalent models at PCC for case 2. (a) Response of real power at bus 8. (b) Response of reactive powers at bus 8. (c) Response of voltage at bus 8. (d) Response of relative rotor angle of SG-2. (e) Response of relative rotor angle SG-3. (f) Response of wind turbine speed. (g) Response of WT Generator speed. (h) Response of WTG torsional angle.

The proposed equivalent model is validated for the following cases:

- Case-1: Three phase to ground fault at bus 8
- Case-2: Rotor speed Instability
- Case-3: Normal operation of the WF

### 6.2.1. Case 1: Three phase to ground fault at bus 8

An average wind speed of 12 m/s is assumed at the first row of detailed system as shown in Figure 4. A three phase to ground fault is applied at the PCC (bus 8) at 1.0 sec and it persists for 0.1 sec. The resulting dynamic responses of real power, reactive power, and voltage

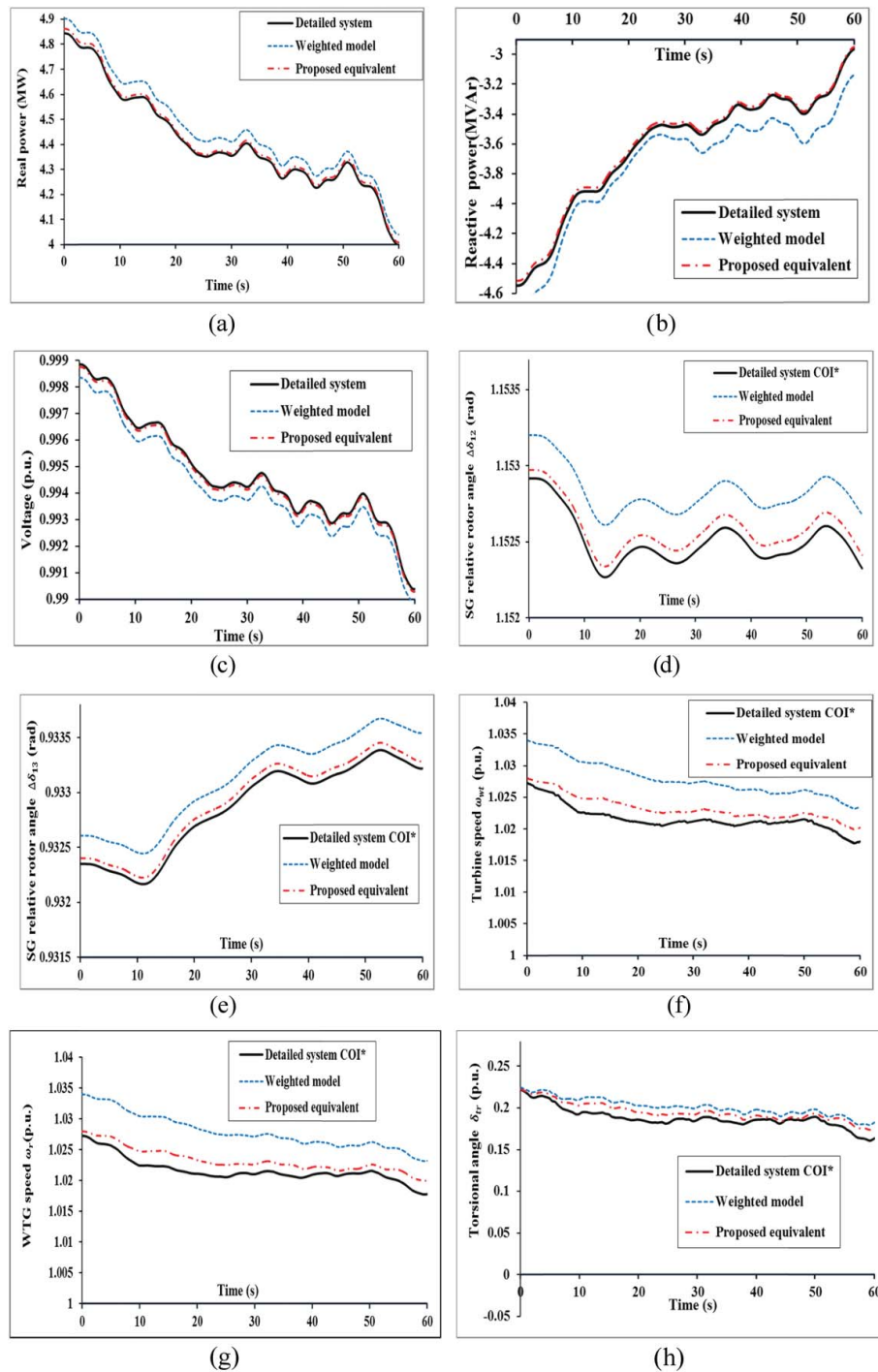


**Figure 9.** Response of the study system and equivalent models at PCC for case 3. (a) Response of real power at bus 8. (b) Response of reactive powers at bus 8. (c) Voltage response at bus 8. (d) Response of relative rotor angle of SG-2. (e) Response of relative rotor angle of SG-3. (f) Response of equivalent wind turbine's speed. (g) Response of WT Generator's speed. (h) Response of WTG torsional angle.

magnitude at bus 8 for the study system with detailed WF representation and WF replaced by equivalent models are shown in Figure 7.

### 6.2.2. Case 2: Rotor speed instability

In this case, the damping of all three SGs is taken as zero. A three phase to ground fault is simulated at bus 8 at 1 sec and removed at 1.1 sec. Due to

insufficient damping of SGs and severe fault leads to growing of oscillations in rotor speed of WTG shown in Figure 8(g)–(h). The impact of the growing of oscillations is reflected on real power, reactive power, and voltage at PCC as shown in Figure 8(a)–(f). This is referred as “rotor speed instability” of WF reported in [28]. The detailed, equivalent model dynamic responses are obtained and compared.



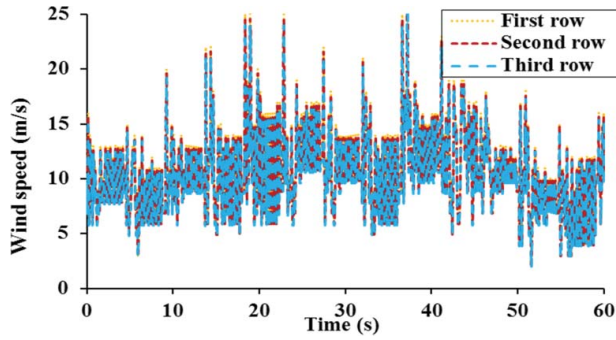


Figure 10. Time series of measured wind speed.

### 6.2.3 Case 3: Normal operation of the wind farm

Under normal operation, the dynamic resulting responses of detailed WF, equivalent by weighted model and proposed are shown in Figure 9. The time series of measured wind speed is considered for this simulation case as shown in Figure 10, applied to detailed WF. The wind speed for proposed equivalent model is calculated as per Equation (30).

### 6.3 Average error between study system with detailed WF and equivalent models

The average error of the responses has been computed for the all the above investigated cases for the detailed system and equivalent models. The average error is expressed as

$$\text{Average error} = \left| \frac{\sum_{i=1}^N (X_{Di} - X_{Ei})}{\sum_{i=1}^N X_{Di}} \right| \times 100. \quad (58)$$

From Table 4, it can be seen that the average deviations in the active power, voltage, rotor angle of SG-2, wind turbine speed, SCIG's rotor speed and it is torsional angle responses between the proposed equivalent and detailed models are less than 1% except for rotor speed instability case, whereas for weighted model the deviations are more. Also proposed equivalent model responses at the PCC are in close agreement with the detailed model responses as shown in Figures 7–9.

Table 4. Average error between study system with detailed WF and equivalent models.

Study cases	Detailed system Vs. equivalent Models	Average error (%)						
		Real power	Reactive power	Voltage	Rotor angle of SG-2	Turbine speed	SCIG rotor speed	WTG torsional angle
1. Three phase to ground fault at bus 8	Weighted model [10]	4.05	5.10	1.17	0.07	0.09	0.21	0.96
	<b>Proposed equivalent</b>	<b>0.90</b>	<b>3.48</b>	<b>0.80</b>	<b>0.03</b>	<b>0.01</b>	<b>0.05</b>	<b>0.10</b>
2. Rotor speed instability	Weighted model [10]	62.87	125.09	8.55	0.17	0.27	0.50	7.74
	<b>Proposed equivalent</b>	<b>21.24</b>	<b>12.98</b>	<b>5.78</b>	<b>0.15</b>	<b>0.07</b>	<b>0.08</b>	<b>2.23</b>
3. Normal wind speed condition	Weighted model [10]	10.25	8.10	9.17	20.07	8.09	7.21	3.96
	<b>Proposed equivalent</b>	<b>1.25</b>	<b>1.58</b>	<b>1.10</b>	<b>4.1</b>	<b>3.3</b>	<b>3.03</b>	<b>1.94</b>

Table 5. Simulation time comparison between study system and equivalent models.

S. no.	Simulation test cases	Simulation time in sec	
		Study system with detailed WF	Proposed and weighted model [10]
1	Three phase to ground fault at bus 8	143.12	17.13
2	Rotor speed instability	154.26	15.45
3	Normal wind speed condition	452.41	83.32

It is inferred from Table 5 that time required to simulate equivalent WF model is very less compared to the study system with detailed WF representation. Hence, the proposed and weighted model equivalent of WF system has significantly reduced the simulation time compared to detailed WF for the time-domain analysis of power system. Processor – Intel® Pentium® – CPU B950 @ 2.10 GHz, 2 GB RAM is used for this simulation.

### 6.4 Comments on equivalent wind farm model

The WTG in a WF may be arranged to be in series or parallel or mixed [29]. In any case, the proposed method can be applied. The impact of the wake effect is observed to be less for the equivalent WF model. This is expected since the single-equivalent generator is compact, whereas the WTGs in the detailed WF are distributed. The eigenvalues of the study system with detail WF representation, WF replaced by proposed equivalent model and weighted model are presented in Tables 2 and 3. The damping and natural frequency of oscillation of proposed equivalent system are very close to detailed WF system when compare to weighted model. In most of the investigated cases, the average error of dynamic responses between the proposed equivalent and detailed models are less when compared to weighted model as shown in Table 4. The equivalent system responses exactly match with detailed system pre-fault conditions, but the response of the weighted model has more deviation during post-fault conditions. But the average error of the dynamic responses of the detailed system and proposed equivalent system are less with acceptable tolerance.

## 7. Conclusion

A method of aggregation of a complex WF that yields a single equivalent is proposed in this paper. The performance of the proposed equivalent is superior to the weighted model equivalent proposed earlier. The dynamic performance of the aggregated equivalent is tested against that of the complex WF. The test involves small- and large-signal disturbances that trigger the electromechanical dynamics. The equivalent WF is obtained by proposed method is also investigated for rotor speed instability case. In addition, the computed eigenvalues and time-domain responses are compared against weighted model.

The eigenvalues obtained from the small-signal study of the proposed equivalent system are very close to detailed WF system than weighted model. Also the time-domain response from the large-signal study reveals that there is a good agreement between the proposed equivalent model and the detailed WF. In some cases, the average error between the detailed and proposed models response is less than 1%. The large-signal responses of the proposed equivalent show significantly superior agreement with detailed system dynamic response compared to weighted model in most of the investigated cases. Future scope of this proposed technique extended to deduce dynamic equivalent of WF with different WTG technologies with suitable assumptions.

## Acknowledgements

The authors thank Dr S. G. Bharathidasan, associate professor of EEE department, S. V. C. E College, Chennai for the help rendered in developing genetic algorithm. The authors also thank management and faculty of Engineering & Technology in SRM University, Kattankulathur for their support and encouragement.

## Disclosure statement

No potential conflict of interest was reported by the authors.

## Nomenclature


$\delta_{sg}$	rotor angle of SG in rad
$\delta_{wt}$	torsional angle between wind turbine and induction generator (IG) in rad
$\lambda$	tip speed ratio
$\Delta$	a change in a variable
$\psi_{ds}, \psi_{dr}$	$d$ -axis stator and rotor flux linages, respectively
$\psi_{qs}, \psi_{qr}$	$q$ -axis stator and rotor flux linages, respectively
$\phi$	pitch angle in radians
$\theta_b$	the angle of bus voltage in rad.
$\theta$	the power factor angle of the equivalent generator.

$\theta_{wt}$	shaft twist angle between wind turbine and generator in rad.
$\rho$	air density in $\text{kg/m}^3$
$A$	area covered by a turbine blade
$C_p(\lambda, \phi)$	performance coefficient of wind turbine
$C_t$	ratio between thrust forces to dynamic force
$C_1 - C_6$	wind wheel constants
$C_e$	compensating capacitor for equivalent generator
$D$	diameter of the wind turbine in meters
$D_{sg}, D_{sh}$	the damping coefficient of SG and wind-turbine generator
$D_{she}$	the damping coefficient of equivalent wind-turbine generator in p.u.
$D_{shemin}, D_{shemax}$	minimum and maximum value of damping coefficient in p.u., respectively
$\overline{E'_m}$	phasor representation of voltage behind transient reactance of IG
$E'_{qs}, E'_{ds}$	$q$ axis and $d$ axis voltage behind transient reactance of IG, respectively
$E'_{sgq}, E'_{sgd}$	$q$ axis and $d$ axis voltage behind transient reactance of SG, respectively
$H_s, H_t, H_g$	inertia constant of SG, wind turbine and IG, respectively
$H_{te}, H_{ge}$	inertia constant of SG, wind turbine and IG, respectively
$H_{temin}, H_{temax}$	minimum and maximum values of inertia constant of wind turbine, respectively
$H_{gemin}, H_{gemax}$	minimum and maximum values of inertia constant of SCIG, respectively
$f$	objective function
$k$	wake decay constant
$K_{sh}$	the shaft stiffness coefficient in Nm/rad
$K_{she}$	the shaft stiffness coefficient of equivalent generator in Nm/rad
$K_{shemin}, K_{shemax}$	shaft stiffness coefficient of equivalent generator in Nm/rad, respectively
$L_s, L_r, L_m$	stator and rotor self-inductance and stator to rotor mutual-inductance in p.u.
$N$	Maximum number of simulation time steps.
$nt$	number of wind-turbine generators
$P$	time-derivative operator $d/dt$
$P, Q$	real power and reactive power, respectively
$\hat{P}_D, P_E$	real power of detailed and equivalent system, respectively
$\hat{Q}_D, Q_E$	reactive power of detailed and equivalent system, respectively
$P_{wte}$	mechanical power of the equivalent wind turbine in p.u.

$R_{sg}$	stator resistance of SG in p.u., respectively
$R$	wind turbine blade radius in meters
$R_s, R_r$	stator and rotor resistance of SCIG in p.u., respectively
$R_{rmin}, R_{rmax}$	minimum and maximum values of rotor resistance of SCIG in p.u., respectively
$I_q, I_d$	quadrature and direct axis current, respectively
$s$	full load slip of the IG
$t$	time in second
$T_{sgm}, T_{sh}$	mechanical torque of SG, shaft torque of IG in p.u., respectively
$T_{sge}$	electrical torque of SG in p.u.
$T_m, T_e$	mechanical torque and electrical torque of WTG in p.u., respectively
$T_o'$	rotor open circuit time constant in sec.
$U_a, U_r(t)$	average and ramp component of wind speed in m/sec, respectively
$U_g(t), U_{tc}(t)$	gust and turbulence component of wind speed in m/sec, respectively
$U_w(t), U_{w2}(t)$	wind speed at first and second wind turbine in m/sec, respectively
$U_{we}, U_{wi}$	wind speed at equivalent generator and $i^{\text{th}}$ WTG in m/sec, respectively
$v_{ds}, i_{ds}$	$d$ -axis stator voltage and current in p.u., respectively
$v_{qs}, i_{qs}$	$q$ -axis stator voltage and current in p.u., respectively
$v_{dr}, i_{dr}$	$d$ -axis rotor voltage and current in p.u., respectively
$v_{qr}, i_{qr}$	$q$ -axis rotor voltage and current in p.u., respectively
$V, \bar{V}_s, \bar{I}_s$	bus voltage and stator voltage phasor, stator current phasor in p.u
$\hat{V}_D, V_E$	voltage of detailed wind farm system and equivalent model, respectively.
$\omega_{sg}, \omega_s$	rotor speed and synchronous speed of SG in p.u.
$\omega_t, \omega_r$	angular speed of the wind turbine and SCIG in p.u.
$X$	distance between two wind turbine rotors in meters.
$X_{WTD}$	distance between two wind turbine rotors in meters.
$X'_q, X'_d$	quadrature and direct axis transient reactance of SG, respectively
$X'_s, X_s, X_r$	stator transient reactance, stator and rotor reactance of IG, respectively
$X_m, X_l$	magnetizing reactance and leakage reactance of IG, respectively
$X_D, X_E$	detailed and equivalent wind farm (WF) parameters.
$[Y]$	admittance matrix of the wind farm

$[Y_{RR}]$	dimension is $1 \times 1$ which corresponds to retained buses after Kron's reduction.
$[Y_{RE}]$	dimension is $1 \times E$ sub matrix of $[Y]$ where $E$ is the number of WF buses eliminated by Kron's reduction.
$[Y_{ER}]$	transpose of $[Y_{RE}]$
$[Y_{EE}]$	dimension is $E \times E$ sub matrix of $[Y]$

## ORCID

Maharajan Duraisamy  <http://orcid.org/0000-0002-8640-5273>

## References

- [1] Zavadil RM, Smith JC. Status of wind-related U.S. national and regional grid code activities. *Power Eng Soc Gen Meeting*. 2005 June 12–16;2:2892–2895.
- [2] Slootweg JG, Kling WL. The impact of large scale wind power generation on power system oscillations. *Electr Pow Syst Res*. 2003 Oct 31;67(1):9–20.
- [3] Akhmatov V, Knudsen H. An aggregate model of a grid-connected, large-scale, offshore wind farm for power stability investigations-importance of windmill mechanical system. *Electr Pow Energy Syst*. 2002;24:709–717.
- [4] Slootweg JG, Kling WL. Aggregated modelling of wind parks in power system dynamics simulations. *IEEE Power Tech Conf*. 2003;3:626–631.
- [5] Shafiu A, Anaya-Lara O, Bathurst G, et al. Aggregated wind turbine models for power system dynamic studies. *Wind Eng*. 2006 May;30(3):171–185.
- [6] Fernandez LM, Saenz JR, Jurado F. Dynamic models of wind farms with fixed speed wind turbines. *Renew Energ*. 2006 Jul 31;31(8):1203–1230.
- [7] Perdana A, Uski—Joutsenvuo S, Carlson O, et al. Comparison of an aggregated model of a wind farm consisting of fixed-speed wind turbines with field measurement. *Wind Energy*. 2008 Jan 1;11(1):13–27.
- [8] Muljadi E, Pasupulati S, Ellis A, et al. Method of equivalent representation for a large wind power plant with multiple turbine representation: preprint. Golden (CO): National Renewable Energy Laboratory (NREL); 2008 Jul 1.
- [9] Li H, Yang C, Zhao B, et al. Aggregated models and transient performances of a mixed wind farm with different wind turbine generator systems. *Electr Pow Syst Res*. 2012;92:1–10.
- [10] Garcia-Gracia Miguel, Comech M. Paz, Sallan Jesus, et al. Modelling wind farms for grid disturbance studies. *Renew Energ*. 2008;33:2109–2121.
- [11] Cheng Xueyang, Lee Wei-Jen, Sahni Mandhir. Dynamic equivalent model development to improve the operation efficiency of wind farm. *IEEE Trans Ind Appl*. 2015. DOI:10.1109/TIA.2016.2537778.
- [12] Yinfeng WA, Chao LU, Lipeng ZH, et al. Comprehensive modeling and parameter identification of wind farms based on wide-area measurement systems. *J Mod Power Syst Clean Energy*. 2016 Jul 1;4(3):383–393.
- [13] Li L, Teng Y, Wang X. Dynamic equivalent modeling of wind farm considering the uncertainty of wind power prediction and a case study. *J Renew Sustain Ener*. 2017 Jan;9(1):013301.

- [14] Rogers J, Manno Di, Alden TH. An aggregate induction motor model for industrial plants. *IEEE Trans Power Apparatus Syst.* 1984;PAS-103(4):683–690.
- [15] Krause PC. *Analysis of electric machinery*. New York: McGraw Hill Inc.; 1986.
- [16] Kundur P. *Power system stability and control*. New York: McGraw-Hill Inc.; 1994.
- [17] Dommel HW. *State-of-the-art of transient stability simulation for electric power system*. California: The University of British Columbia; May 1976.
- [18] Ramanujam R. *Power system dynamics: analysis and simulation*. Chennai: PHI Learning Private Ltd.; 2013.
- [19] Lubosny Z. *Wind turbine operation in electric power systems: advanced modeling*. Berlin: Springer; 2003.
- [20] Jensen NO. *A note on wind generator interaction*. Roskilde: Riso National Laboratory; 1983.
- [21] Johnson Gary L. *Wind energy systems*. Electronic Edition ed. Manhattan (KS): Prentice Hall Inc.; 2006.
- [22] Mercado-Vargas MJ, Gomez-Lorente D, Rabaza O, et al. Aggregated models of permanent magnet synchronous generators wind farms. *Renew Energ.* 2015 Nov 30;83:1287–1298.
- [23] Abledu KO. *Equivalent load model of induction machines connected to a common bus*. [Retrospective Theses and Dissertations]. Ames (IA): Iowa State University; 1983.
- [24] Qiao Jia-Geng, Lu Zong-Xiang, Min Yong. A novel dynamic equivalence method for grid-connected wind farm. *J Zhejiang Univ Sci A.* 2008;9:558–563.
- [25] Liu B. *Theory and practice of uncertain programming*. New York (NY): Physica-Verlag; 2002.
- [26] Pai MA, Gupta DP Sen, Padiyar KR. *Small signal analysis of power systems*. Urbana: Narosa Publishing House; 2004 Aug 1.
- [27] Matlab. *The matrix laboratory*. Natick: The Math Works Inc.; 2013.
- [28] Jayashri R, Kumudini Devi RP. Effect of tuned unified power flow controller to mitigate the rotor speed instability of fixed-speed wind turbines. *Renew Energ.* 2009;34:591–596.
- [29] Bansal R. editor. *Handbook of distributed generation: electric power technologies, economics and environmental impacts*. Pretoria: Springer; 2017 Apr 9.

## Appendix

### Study system parameters

#### A.1 Wind turbine data

Rated wind speed:	Cut in wind speed:	3 m/s
12 m/s		
Cut out wind speed:	Specific air density ( $\rho$ ):	1.06 kg/m <sup>3</sup>
22 m/s		
Gear box ratio $b$ :	Blade radius $R$ :	26.1 m
1: 67.5		
Wind wheel coefficients and constant ( $x$ ):	$C_1 = 0.5$ ; $C_2 = 67.56$ ; $C_3 = C_4 = 0$ ; $C_5 = 1.517$ ; $C_6 = 16.286$ ;	Pitch angle ( $\theta$ ): 0 deg
	$x = 0$	

**Table A.1.** Reactive power compensation

WTG real power generation in %	kVAr compensation	
	Max kVAr	Min kVAr
Average	98	33
25%	87.5	25
50%	100	37.5
100%	112.5	37.5

**Table A.2.** Study system transmission line and transformer parameters

Transmission line parameters	Voltage		Transformer name	Power rating MVA	Voltage level kV		%Z
	230 kV	11 kV					
Resistance (ohm/km/ckt)	0.0024	0.13	T1	0.5	11/0.433	2.5	
Reactance (ohm/km/ckt)	0.4927	0.0952	T2	1	11/0.433	5.7	
Susceptances (mho/km/ckt)	5e-6	$2 e^{-6}$	TT1 to TT4	250	15.75/230	15	

**Table A.3.** Maximum and minimum values of GA control variables

Limits (p.u.)	Rotor resistance ( $R_r$ )	Turbine inertia ( $H_{te}$ )	Generator inertia ( $H_{ge}$ )	Damping coefficient ( $D_{she}$ )	Stiffness coefficient ( $K_{she}$ )
Maximum	5.00	10	1	1	2.0
Minimum	0.0264	5.0	0.5	0.5	1.0

**Table A.4.** Genetic algorithm parameters

Parameters	Values/types
Population size	30
Cross over probability	0.85
Cross over	Intermediate cross-over
Mutation probability	0.05
Mutation	Element wise mutation
Maximum number of iterations	85